Eur Biophys J (1991) 20:17–29

European Biophysics Journal

Modelling mechanosensitivity in membranes: effects of lateral tension on ionic pores in a microcystin toxin-containing membrane

A. G. Petrov [1,*], R. L. Ramsey [1], G. A. Codd [2], and P. N. R. Usherwood [1]

[1] Zoology Department, University of Nottingham, University Park, Nottingham NG7 2RD, United Kingdom
[2] Department of Biological Sciences, University of Dundee, Dundee, DD1 4HN, United Kingdom

Received January 10, 1991/Accepted in revised form March 27, 1991

Abstract. Lipid bilayers of diphytanoyl lecithin (DPhL) in which a cyanobacterial toxin, microcystin-LR (MC-LR) was incorporated, were found to be a convenient model of natural mechanosensitive membranes. The effects of pressure difference, leading to lateral membrane tension, on artificial membranes formed on the tips of glass micropipettes were investigated using patch-clamp methodology. Emplacement of MC-LR from the bathing solution was enhanced by transmembrane voltage and/or pressure difference. MC-LR pores could be recorded over a wide voltage range, their opening probability being first increased and then reduced at high membrane potential. The pores exhibited several open pore conductance levels, the higher conductance states being more probable at greater lateral tensions. Ion gradient experiments established that the MC-LR pores are cation selective, but discriminate only weakly between K and Na. These results suggest that a lipid liquid crystal matrix containing monomers of multimeric pore-forming molecules could be used as a mechanical sensor and molecular switch.

Key words: Mechanosensitivity – Patch clamp – Diphytanoyl lecithin – Cyanobacteria – *Microcystis* – Microcystin-LR – Ion channels – Membrane lateral tension – Lipid/toxin model membranes – Molecular switches – Molecular electronics

1 Introduction

Mechanosensitivity or mechanotransduction is a property of importance to both animals and plants. The discovery that membranes respond to mechanical tension by an increase in ion permeability was made by Katz (1950) and suggestions that ion channels might be involved were initially made by Edwards et al. (1981) and Corey and Hudspeth (1983). Stress-activated (SA) membrane channels were first discovered in 1984 (Brehm et al. 1984; Guharay and Sachs 1984) and their presence in more than 30 membrane types has been subsequently established (Sachs 1988; Morris 1990). Recently, Morris and Sigurdson (1989) have discovered stress-inactivated (SI) ion channels coexisting with SA ion channels.

In order to explain the high stretch sensitivity of SA channels, Guharay and Sachs (1984) and Sachs (1986, 1988) proposed that the submembranous cytoskeleton plays an active role in membrane mechanosensitivity. The cytoskeleton meshwork is thought to collect stress from large areas of the membrane and to concentrate it in the channels that are "anchored" in the bilayer. If the state of the meshwork is under metabolic control this mechanism raises the possibility of physiological regulation of stress sensitivity (Sachs 1986). To obtain a better insight into membrane mechanosensitivity a reductionistic approach involving model membranes might be useful. Also, such model membranes could serve as interesting prototypes of molecular devices capable of mechanotransduction.

Higher lateral tension can induce ion-conductive pores in pure lipid bilayers, but the appearance of these pores is usually a precursor of irreversible membrane rupture (for review see e.g. Petrov et al. 1980). Permeability changes of black lipid membranes (BLM), modified with dibarenyl mercury, accompaning periodical expansion have been reported by Passechnik and Sokolov (1973). Artificial membranes containing reconstituted ion channels, particularly if they are stress-sensitive in vivo could, in principle, provide excellent working models. However, purified SA channels are not yet available, so this approach remains hypothetical. Other channel-formers, such as low molecular weight peptides provide an interesting alternative to protein channels and this is the approach adopted in this paper. The absence of cytoskeleton proteins in artificial lipid/peptide membranes simplifies interpretation of stress-activated phenomena in this type of membrane system.

* *Permanent address:* Laboratory of Liquid Crystals and Molecular Electronics, Institute of Solid State Physics, BG-Sofia 1784, Bulgaria
Offprint requests to: P. N. R. Usherwood

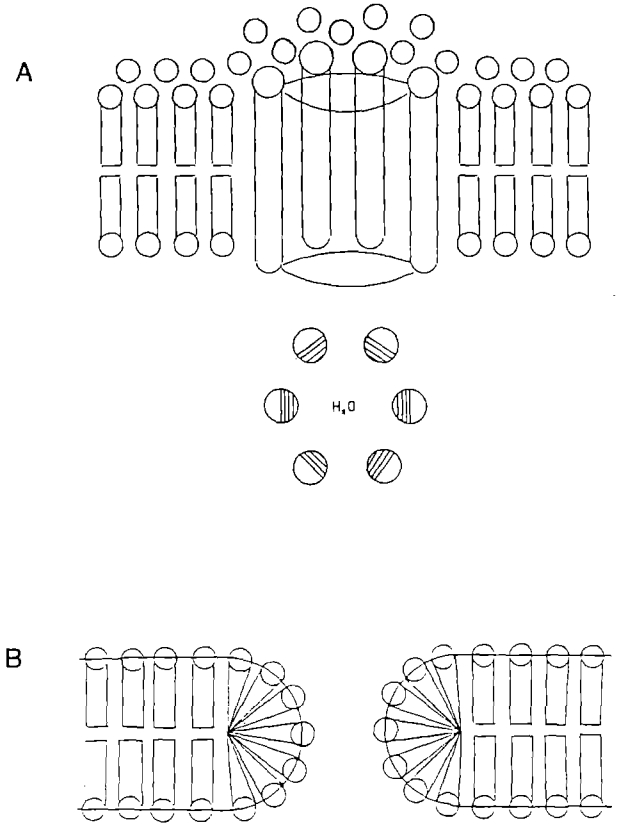

Fig. 1 A, B. Two types of aggregation of defect-forming molecules (peptides) in lipid bilayer membranes determined according to shape asymmetry and biphilic asymmetry: **A** channel; an aggregate of cylindric molecules featuring transverse biphilic asymmetry (hydrophilic portions hatched in surface view illustrated below). Molecular length should roughly match the bilayer thickness. **B** pore; an aggregate of wedge-shaped molecules featuring longitudinal biphilic asymmetry. Molecular length should roughly match half of a bilayer thickness

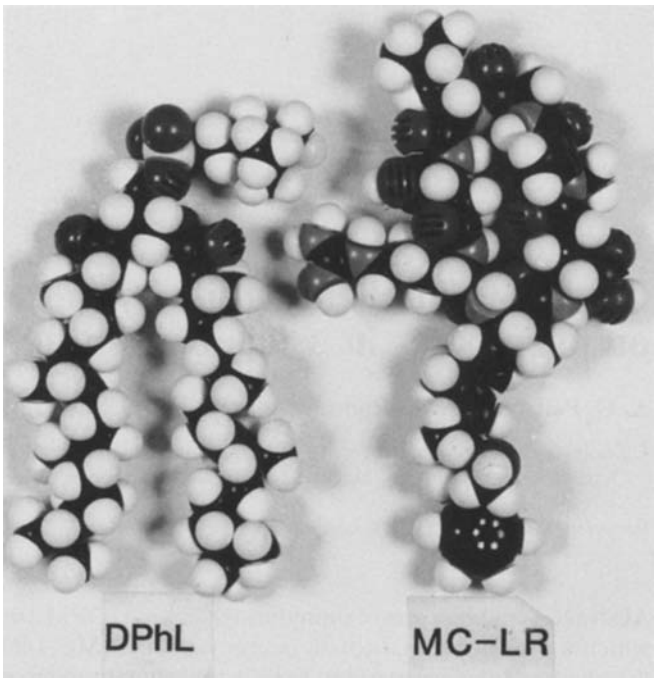

Fig. 2. Comparison of space-filling models of the bilayer-forming lipid, diphytanoyl lecithin (DPhL, left) and the pore forming peptide, mycrocystin-LR (MC-LR, right). Phytanoyl chains of DPhL are shown in a disordered, 'fluid' conformation. MC-LR conformation is according to the amino acid sequence of Botes et al. (1985) and Krishnamurthy et al. (1989). Note that the lengths of the hydrophobic portions of both molecules almost match. The hydrophilic part of MC-LR is much bulkier than that of DPhL; therefore, the wedge shape of MC-LR could lead to a pore type of aggregation in a bilayer (Fig. 1 B)

Microcystin is a generic term for at least 10 cyclic peptide toxins produced by cyanobacteria (blue-green algae). These toxins have contributed to a world-wide incidence of animal poisonings, and to human health problems, associated with toxic cyanobacterial blooms (Carmichael 1989; Codd et al. 1989 a). The toxins consist of 7 amino acids, two of which are variable, with the hydrophobic β-amino acid residue of 3-amino-9-methoxy-2,6,8-trimethyl-10-phenyldeca-4,6-dienoic acid (Adda) invariably being present. Microcystin-LR (MC-LR), the toxin used in the present study is one such toxin (Botes et al. 1985; Krishnamurthy et al. 1989). If ingested by mammals, or administered intraperitoneally, MC-LR causes extensive liver damage (loss of lobular and sinusoidal architecture with hepatocyte necrosis and massive pooling of blood in the liver) with death due to haemodynamic shock and heart failure (see Carmichael 1989; Codd et al. 1989 a). Cellular damage by MC-LR includes deformation of cell shape with bleb-formation, particularly in hepatocytes, with loss in respiratory capacity, enzyme leakage and cytoskeletal microfilament reorganisation (Falconer and Runnegar 1987; Eriksson et al. 1988, 1989; Codd et al. 1989 b). A significant increase in both cation and anion efflux at toxin concentrations as low as 1 nM has been found (Eriksson et al. 1987).

Quite surprisingly, we have found the MC-LR induces tension-sensitive ion channels in model lecithin membranes.

The usual way of inducing lateral stress in membrane experiments is to impose a pressure difference across the membrane. For closed membrane systems, like vesicles or cells, this is best achieved using osmotic pressure differences, but for planar lipid bilayers hydrostatic pressure is a more relevant option.

Let us now consider lipid/peptide model membranes with multimeric ion channels formed by aggregation of peptide monomers. Depending on the biphilic asymmetry and shape asymmetry of the peptides (Derzhanski and Petrov 1982; Petrov and Derzhanski 1987; Petrov 1988) two limiting types of peptide aggregates could be expected (Fig. 1): cylindrical and semi-toroidal. The former are likely to be formed by roughly cylindric peptides with hydrophilic groups located on one side of the cylinder surface only (e.g. alamethicin, δ-toxin etc.) (Fig. 1 A). The latter are to be expected for wedge-shaped peptides with hydrophilic groups located on the thicker end of the wedge (Fig. 1 B). We will designate the first type as a channel and the second type as a pore. Intermediate types of aggregates are also possible. According to the molecular model of MC-LR (Fig. 2) multimers with the structure of pores are to be expected with this toxin.

The influence of tension on a pore can be discussed in terms of one basic pore parameter i.e. the edge energy of the pore periphery $\gamma(R)$ (Petrov et al. 1980). This energy is related to the radius of the pore according to a series expansion:

$$\gamma(R)=\gamma_0+\gamma_1/R+\gamma_2/R^2. \quad (1)$$

Note that with toroidal pores, R is the radius measured with respect to the torus axis (Fig. 1 B). For cylindrical channels the origin of the increase of edge energy seen with decreasing pore radius can be sought in the "hydration force" resisting the extrusion of water from the channel interior. In pores, additional contributions may arise from the curvature and saddle curvature energy of the edge. More specific molecular models could provide values for γ_0, γ_1 and γ_2 (Petrov et al. 1980; Pastushenko and Petrov 1984).

By minimizing the total pore energy $2\pi\gamma(R)\cdot R$ with respect to the radius an equilibrium radius can be found:

$$R_0=\sqrt{\gamma_2/\gamma_0}. \quad (2)$$

With a low lateral tension σ, the dependence of this radius on tension can be obtained on the basis of an additional contribution of the kind described in the linear model presented above: an area increase directly coupled to lateral tension. The total pore energy is now:

$$E(R)=2\pi\gamma_0 R+2\pi\gamma_1+2\pi\gamma_2/R-\pi R^2\sigma. \quad (3)$$

By minimizing it with respect to R, one obtains a cubic equation for the equilibrium radius. An approximate solution of this equation in the limit of low σ is obtained by representing

$$R(\sigma)=R_0+\Delta R(\sigma) \quad (4)$$

where R_0 is the radius with zero tension (9) and ΔR is

$$\Delta R=\frac{\sigma R_0^2}{2\gamma_0-3\sigma R_0}. \quad (5)$$

When the tension is low, ΔR increases linearly with σ; when it approaches a critical tension of

$$\sigma_{cr}=2\gamma_0/3R_0 \quad (6)$$

an irreversible growth of the pore results and the membrane proceeds to mechanical breakdown, or lysis. A typical value for the edge energy of a pure lipid bilayer is $2\cdot10^{-11}$ N. Wedge-like molecules concentrated in the edge tend to decrease this energy (Petrov et al. 1980). With a pore radius of 1 nm the critical tension from (13) is of the order of 10 mN m^{-1}. If the initial pore radius is small then the concentration of ions within it may be vanishingly low, because of the steep increase of ion chemical potential in narrow pores (see Pastushenko and Petrov 1984). As a result the pore may be nonconducting. In the description of edge energy presented above the pore radius is continuously variable. In reality the increase of the pore radius is not smooth but stepwise, because each change in radius will require an increase of one in the number of molecules forming the pore. Thus, pore gating by voltage and tension may be better described in terms of a discrete stochastic approach based on the nucleation theory of bilayer stability (Exerowa and Kashchiev 1986) and its extension for the case of an applied electric field, the stochastic model of electric field-induced membrane pores (Sugar 1989). Such an approach, however, has not yet been developed for the case of bilayers containing two types of lipids with different shape asymmetry. Discrete radii increments of a pore could be responsible for the sudden transitions from closed to open state and to higher conductance open states. Charged groups on the channel and pore surface may control the ion selectivity of a pore.

2 Materials and methods

The purified cyanobacterial toxin, MC-LR (mol wt 994 Da) was isolated from *Microcystis aeruginosa* strain PCC 7820 according to Brooks and Codd (1986) with confirmation using a Waters 991 photodiode array detector. It was dissolved in methanol (AR grade, Fisons) and kept at −20 °C. The toxin is a cyclic peptide with 7 amino acid residues, viz. cyclo-(D-Ala-L-Leu-*erythro*-β-methyl-Asp-Arg-Adda-D-Glu-N-methyldehydro-Ala) (Carmichael 1989; Eriksson et al. 1987). Among these residues is a novel β-amino acid, Adda, with an unsaturated side chain, which, apart from containing a methoxy group, is markedly hydrophobic (Fig. 2).

Lipid bilayers were formed using diphytanoyl lecithin i.e. 3,7,11,15-tetramethylhexadecanoyl lecithin (DPhL), mol wt 846.27 Da (Avanti Polar Lipids, Birmingham, Alabama). Due to its branched alkyl chains, this lipid is in a liquid crystal state at room temperature (22 °C, i.e. the temperature at which the experiments were undertaken) and it does not display a phase transition to the gel state until −120 °C (Lindsey et al. 1979). A comparison of space-filling molecular models of DPhL and MC-LR (Fig. 2) demonstrates that the hydrophobic moieties of these molecules are almost equal in length (DPhL chains shown in a 'fluid' conformation). Judging from the molecular asymmetry of MC-LR, a pore type of aggregation in DPhL bilayers is conceivable (see Discussion).

The buffer used in most cases was 150 m*M* KCl (FSA Lab. Suppl.), 10 m*M* BES (Sigma), pH 7.0. Experiments aimed at establishing the ion selectivity of the MC-LR channels were performed under ion gradient conditions using KCl and NaCl buffers of various concentrations (see below).

Lipid bilayers were formed at the tips of patch pipettes from lipid monolayers spread on an air/water interface by the method of Corronado and Latorre (1983). A solution of DPhL in either chloroform (10 mg ml^{-1}) or *n*-pentane (10 mg ml^{-1} or 1 mg ml^{-1}) was employed. The pipettes were pulled from thick walled borosilicate glass (GC150-10, Clark Electromedical Instruments) on a modified horizontal puller (Industrial Science Associates) or a modified vertical puller, Model 700C (David Kopf Instruments). When filled with 150 m*M* KCl buffer, the pipettes had resistances in the range 1–4 *M*Ω, which correspond to tip diameters of 2–4 μm (Sakmann and Neher 1983). The large tip diameters were expected to enhance the amount of lateral tension in the bilayer at lower pressure

differences according to the Laplace law for a hemispherical patch at a pipette tip (Sachs 1988). Disposable Petri dishes of 10 cm^2, 20 cm^2 and 60 cm^2 area were filled with 5 ml, 5 ml and 18 ml buffer, respectively. A lipid solution of typically 1 µl volume (10 mg ml^{-1} concentration) or 10 µl (1 mg ml^{-1} concentration) was spread over the electrolyte surface using a Hamilton syringe. Lipid spreading was monitored by a Leitz inverted, phase contrast microscope with an attached colour video camera, VK-C150ED (Hitachi). Larger areas of buffer surface and higher concentrations of lipid were used in an attempt to minimize the number of the solvent droplets which were often found on the buffer surface many hours after spreading of the lipid. Surface pressure and thus the surface packing density of the lipid monolayer was controlled in separate experiments by means of a torsion balance (White model) by measuring (using a filter paper strip) the fall in surface tension of the buffer produced by spreading a given amount of lipid.

The seal resistance of the formed bilayers was typically a few tens of gigaohms. The bilayers were exposed to MC-LR added to the pipette-filling electrolyte or, in some cases, to the bathing electrolyte as a methanol solution to a final concentration in the buffer ranging from 10 ng ml^{-1} up to 200 ng ml^{-1}. Emplacement of the toxin was facilitated by briefly raising the membrane potential to −200 mV (MC-LR in the pipette) or 200 mV (MC-LR in the bath) and/or by mechanical stressing the bilayer.

Membrane potentials by convention bear the sign of the electrode inside the pipette; thus positive potentials correspond to currents flowing out of the pipette, pore openings being plotted upwards on the text-figures. Pressure differences are similarly identified as positive when the pressure inside the pipette is higher than outside (blowing of the bilayer) and negative in the opposite case (sucking of the bilayer). Constant and variable pressures (pressure ramps) were created by a reversible peristaltic pump (Camlab) and monitored by a pressure meter which was a bridge based on a MPX100AP (Motorola) silicon piezoresistive pressure sensor. It provided an accurate, linear voltage output which was directly proportional to the applied pressure. It was calibrated against a mercury manometer to provide an output of 1 mV $torr^{-1}$.

Pore activity was recorded using a List EPC7 patch-clamp amplifier (List-Electronic, Darmstadt) with current and voltage output directed either to a modified Sony PCM linked to a standard video recorder or to a four-channel RACAL Store-4 tape recorder. Simultaneous recording of the pressure signal was also made on a RACAL tape recorder. Stimulating voltages of various waveforms and slow voltage ramps were generated by a VCF/sweep generator, Model 126 (Exact).

Data analysis was undertaken on a Masscomp MC5500 computer. Recordings of membrane currents were low-pass filtered at 1–3 kHz on playback and A/D converted at 10 kHz. Current amplitude distributions were obtained and fitted as described in Mellor et al. (1988). Analysis of pore gating in response to voltage ramps was performed by the method of current-voltage surfaces (Sansom and Mellor 1990). Pore gating kinetics were studied by constructing probability density functions (pdfs) (as in Kerry et al. 1987), from pore current records reduced to vectors of pore dwell times using a single-threshold crossing algorithm (Kerry et al. 1987).

3 Results

3.1 MC-LR does create pores in lipid bilayers

The pore forming action of MC-LR is best demonstrated when the toxin is added to a preformed lipid bilayer which does not exhibit pore openings in the absence of toxin. Figure 3 reports the result of such an experiment. After recording the membrane current response to a slow voltage ramp (1.5 mV s^{-1}; ±100 mV) the toxin was added to the bathing electrolyte to give a concentration of 20 ng ml^{-1}. Initially, no pore openings were observed (Fig. 3A). Successful MC-LR emplacement was accomplished only by raising the steady-state (d.c.) membrane potential to 200 mV. After about 15 s, large conductance pore openings were observed. If the d.c. voltage was brought back to zero and the ramp then restarted, the current trace was remarkably different than before (see the inset of Fig. 3B). Current-voltage surfaces from the membrane now exhibited as many as 8 discrete conductance levels ranging from 150 to 1800 pS (Fig. 3B). Pore gating seemed to be voltage-dependent: at zero membrane potential open pores were mainly absent. The number of open pore conductance states was larger at negative than at positive voltages. Somewhat surprisingly, a small negative current was sometimes observed at 0 mV when toxin was emplaced.

Another example of MC-LR emplacement, this time from the pipette-filled solution, is shown in Fig. 4. In this case it was achieved at a membrane potential of −200 mV, which was typical for toxin emplacement from the pipette side of the membrane. Figure 4 demonstrates the appearance of brief currents signalling the initial stage of pore formation by MC-LR.

3.2 MC-LR is weakly surface active.

Surface tension measurements gave an idea of the surface activity of MC-LR in comparison to the lipid DPhL. Spreading 10 µl of 1 mg ml^{-1} MC-LR in MeOH over a 10 cm^2 Petri dish resulted in a fall in surface tension of the 150 m*M* KCl buffer of 2.5 mN m^{-1}. Addition of another 10 µl of MC-LR reduced surface tension by 1 mN m^{-1}. Presumably, most of the MC-LR dissolves in the buffer and its surface density is low. In contrast, when pipetting pure MeOH onto the buffer surface, a fall in surface tension of 1 mN m^{-1} was obtained with only 60 µl of the alcohol. When 1 µl of 10 mg/ml^{-1} DPhL solution in chloroform (a solution in which the number of DPhL molecules was about the same as the number of MC-LR molecules in the toxin solution) was spread on the buffer surface, a 49 mN m^{-1} fall in surface tension was observed. The lipid produces a tightly packed monolayer of 49 mN m^{-1} surface pressure because DPhL is practically insoluble in water. When the same amount of DPhL was spread from a pentane solution (10 µl of 1 mg ml^{-1}), a

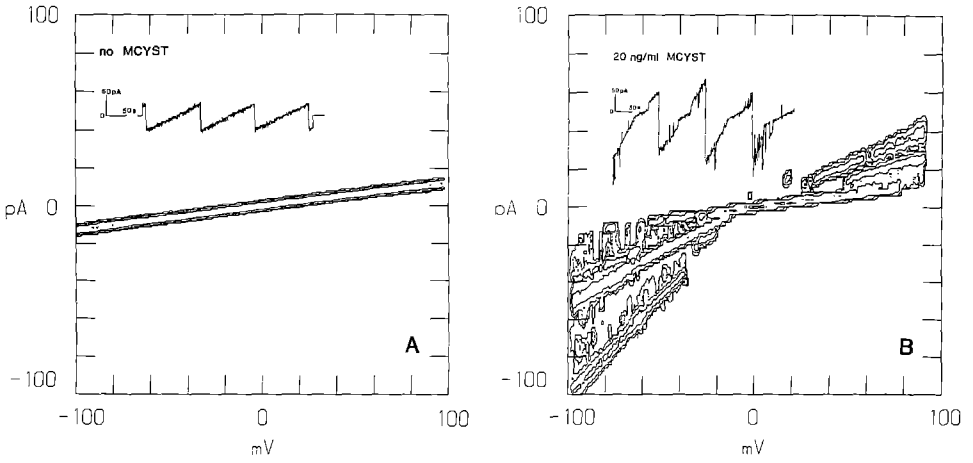

Fig. 3. Current-voltage surfaces of **A** a pure DPhL bilayer and **B** of the same bilayer exposed to MC-LR added to the bath to give a final concentration of 20 ng ml^{-1}. Ordinates, membrane current; abscissae, ramp voltage. Both recordings at 0 torr. I/V surfaces were averaged over 5 successive ramps. Pipette resistance, 1 $M\Omega$ (150 m*M* KCl). 1 µl of 10 mg ml^{-1} DPhL/pentane spread over 10 cm^2 petri dish; seal resistance, 8 GΩ; −100 mV to 90 mV voltage ramp, during 132 s. Insets are current traces produced by the voltage ramp. In **B** note discrete pore conductance states emerging after adding 10 µl of 10 µg ml^{-1} MC-LR-methanol to the 5 ml of bathing electrolyte and briefly increasing the membrane potential to 200 mV. Conductance states of 151 pS, 283 pS, 382 pS, 604 pS, 922 pS, 1.1 nS, 1.6 nS and 1.8 nS (not shown) were identified

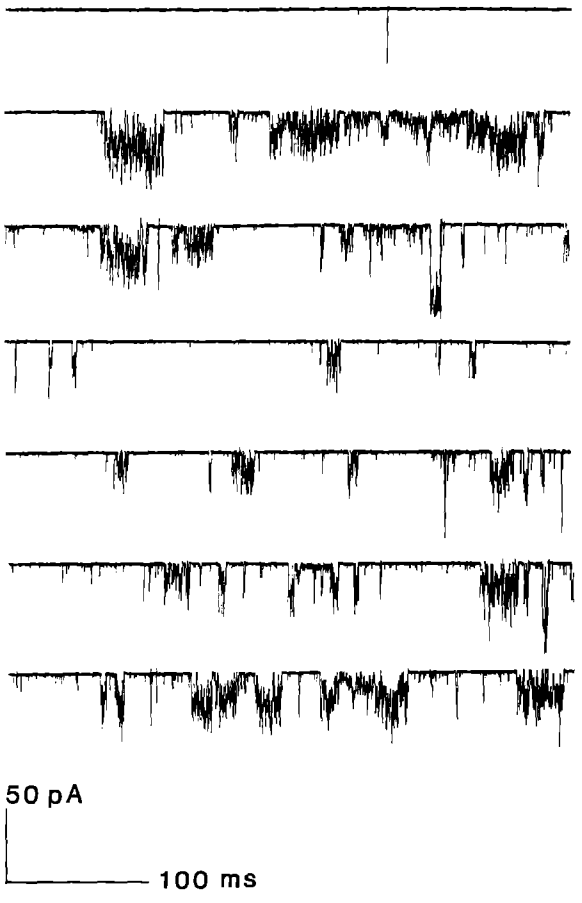

Fig. 4. Membrane currents observed during the initial period of MC-LR (10 ng ml^{-1}) emplacement from the pipette to a bilayer at −200 mV membrane potential and 0 torr pressure difference. Pipette resistance, 10 $M\Omega$ (100 m*M* KCl buffer); seal resistance, ca 100 GΩ. 1.5 µl of 10 mg ml^{-1} DPhL/chloroform spread over 20 cm^2 petri dish. Monolayer surface pressure 43 mN ml^{-1} (see Materials and Methods). 10 ng ml^{-1} MC-LR in pipette buffer. Successive traces are shown starting from the moment of voltage application

lower surface pressure monolayer (37 mN m^{-1}) resulted. The lower packing density in this case may have been due to the larger number of nonspreading solvent microdroplets which could be readily visualised by phase contrast microscopy. Addition of the same amount of MC-LR in MeOH solution (10 µl of 1 mg ml^{-1}) to this monolayer decreased its surface tension by 2.5 mN m^{-1}, indicating additivity of surface pressure in a mixed monolayer.

The final concentration of MC-LR in the buffer (buffer volume of 5 ml) in the above experiments was 2 µg ml^{-1}, i.e. 100 times higher than the typical concentration employed in pore-forming experiments. There was no measurable change in surface tension following spreading of 10 µl of 10 µg ml^{-1} MC-LR solution; with 20 µl it fell by 0.25 mN m^{-1}, but this change may have been due to the MeOH solvent.

3.3 Toxin emplacement depends on monolayer lipid packing density

By varying the amount of lipid spread and the area of the buffer surface, monolayers with various surface pressures could be prepared. For example, with 20 cm^2 dishes and 10 mg ml^{-1} DPhL-chloroform solution spreading of lipid in volumes ranging from 0.5 to 2 µl resulted in surface pressures in the range 25–50 mN m^{-1}; 1 mg ml^{-1} DPhL/pentane solutions, in volumes ranging from 5 to 20 µl, resulted in surface pressures in the range 15–45 mN m^{-1}. These data were prone to substantial scatter due to volume errors. The errors were largest with concentrated lipid solutions, which may have been due to incomplete spreading of the lipid as mentioned previously. When spreading from chloroform, the surface pressure of a monolayer equilibrated at least twice as quickly as when spreading from pentane. The use of phase-contrast video microscopy enabled us to select monolayer areas free of droplets for bilayer formation.

A general finding was that the seal resistance of a membrane patch was directly proportional to the surface pressure of a monolayer; in the upper range of pressures (45–50 mN m^{-1}), the seal resistance could be as high as 100 GΩ. On the other hand, GΩ seals could not be formed below 15 mN m^{-1}. With respect to MC-LR emplacement, spontaneous pore activity (i.e. at 0 torr and 0 mV) was often observed with surface pressures of about 20–25 mN m^{-1}. With membranes formed from monolayers of higher surface pressures, either transmembrane potential or pressure application was required to achieve MC-LR emplacement. However, in the upper limit of 50 mN m^{-1} surface pressure ±200 mV alone was insufficient for pore formation, although pore formation (MC-LR emplacement?) could be achieved if negative lateral tension was simultaneously applied by sucking the membrane patch. The π-A isotherm of DPhL has not been obtained, but judging from other double-chained lecithins (Albrecht et al. 1978) a 50 mN m^{-1} surface pressure results in a tightly packed monolayer; native membranes have lateral pressures of about 25 mN m^{-1}, so the packing of lipids is less tight.

3.4 MC-LR pores are stress sensitive

Figure 5 shows the result of a pressure experiment following MC-LR emplacement in the membrane of Fig. 4. Reducing the voltage to zero closed the MC-LR pore and voltages of ±100 mV did not result in pore openings. However, pore openings were obtained by clamping the voltage at −100 mV and gradually raising the suction pressure to −60 torr. The pressure was kept at this level for 15 s and from the pore current fluctuations a histogram was prepared which gave a single, open pore conductance of 67.4±4.7 pS (Fig. 5 A). Interestingly, after releasing the pressure to zero the pore remained open for some minutes (Fig. 5 B) before eventually closing.

The effects of negative pressure on opening of a pore were studied using a combination of voltage ramp and steady state pressure. Current-voltage surfaces of a MC-LR containing membrane for various negative pressures were obtained. In Fig. 6 the threshold for pore opening at −110 mV was −11 torr. Voltage and lateral tension acted in concert: higher conductance states occurred at increasingly lower voltages as the pressure was increased. They were also more abundant at negative pipette potentials. At −50 torr, 3 conductance states at negative voltages and 2 at positive voltages were identified by measuring the slopes of the lines drawn along the centres of the contours in Fig. 6 D, with respect to the closed pore state (not shown). Somewhat surprisingly, there was a tendency for tension-induced, open conductance states to be replaced by lower conductance states at high voltages: the solid contours on Fig. 6 D, surrounding an area containing the second largest number of pore events (100), become discontinuous (island-like) and eventually terminate at high negative and high positive voltages. This feature was apparent in many recordings (see below).

3.5 MC-LR pores are cation-selective but only weakly K/Na selective

In order to establish ion selectivity of the MC-LR-induced pores, experiments were undertaken to determine the reversal voltage from the pore currents under various transmembrane ion gradients. Cation versus anion selectivity was established by means of a 6-fold KCl gradient, i.e. 500 m*M* KCl outside and 83 m*M* KCl inside the pipette. Averaged current-voltage curves for this condition are displayed in Fig. 7. They were obtained in response to a triangular voltage change of ±200 mV and various pressures. With zero pressure, initially no pore openings could be obtained; only a leak current was recorded which was reversed at 19 mV (arrow 1). To induce pores,

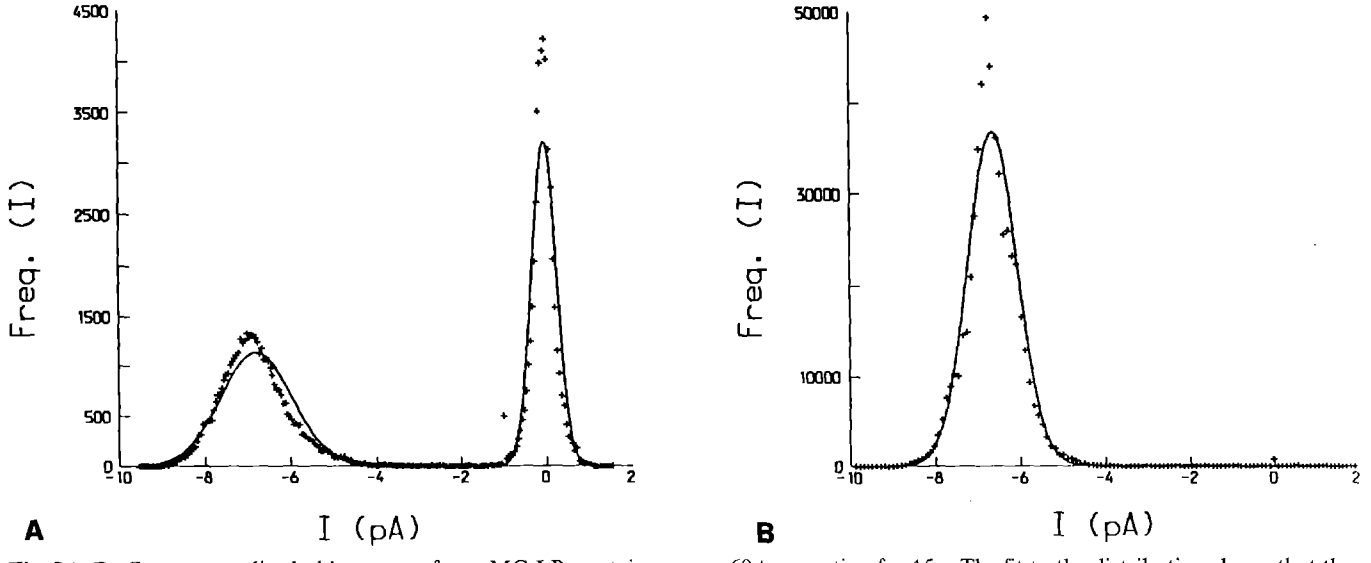

Fig. 5 A, B. Current amplitude histograms for a MC-LR-containing bilayer demonstrating the effect of pressure at a membrane potential of −100 mV. Experimental conditions identical to those of Fig. 4. **A**, a 67.4±7.4 pS open pore state appeared after applying −60 torr suction for 15 s. The fit to the distribution shows that the open state probability is 0.5. After releasing the pressure the pore was mainly open **B**, transitions to the closed state being rare. The bin width was 0.1 pA for **A** and **B**

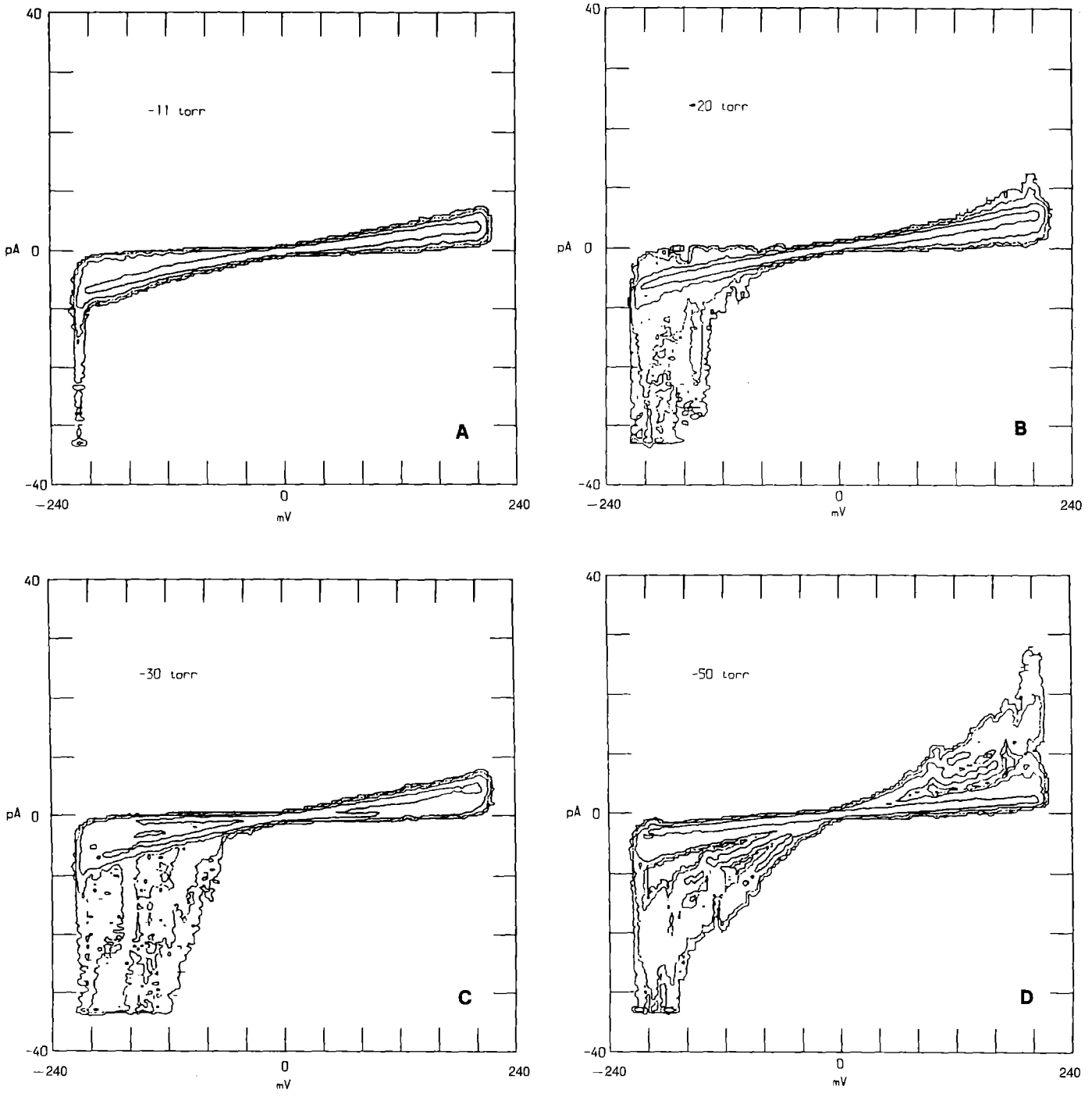

Fig. 6A–D. Progressive opening of higher conductance pore states under suction. Voltage ramp about −210 mV to 210 mV, duration 10 s, Data averaged over 15 successive ramps. Current-voltage surfaces of a MC-LR-containing bilayer at −11 torr (**A**), −20 torr (**B**), −30 torr (**C**) and −50 torr (**D**). Ordinates, membrane current; abscissae, ramp voltage. Pipette resistance, 5 $M\Omega$ (100 mM KCl buffer); seal resistance, 40 GΩ. 1.5 µl of 10 mg/ml^{-1} DPhL/chloroform spread over 20 cm^2 Petri dish. 10 ng ml^{-1} MC-LR in pipette buffer. At −50 torr, 3 conductance states at negative potentials (88 pS, 147 pS and 220 pS) and 2 conductance states at positive potentials (71 pS and 119 pS) can be identified

a positive pressure was applied first. This pressure produced first an increase of seal resistance, which was maximal at 120 torr (Fig. 7A), followed by a decrease in resistance. At 130 torr, pore openings started to appear. Negative pressures also had a threshold for pore opening (Fig. 8) of about −120 torr. For both positive and negative pressures the reversal voltage of the pore current was positive, its average value being 37.5 mV. Using the Goldman-Hodgkin-Katz equation (Hille 1984, Eq. 10–14), a ratio of the permeabilities of chloride and potassium was obtained viz:

$$P_{Cl}/P_K = 0.175,$$

i.e. a high cation selectivity. Note again in Fig. 8 the switching of high conductance states to lower ones at both high positive and high negative voltages. This phe-

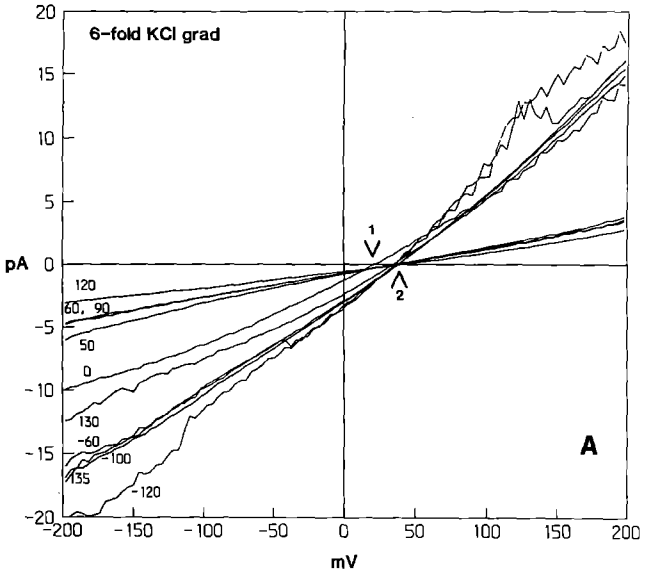

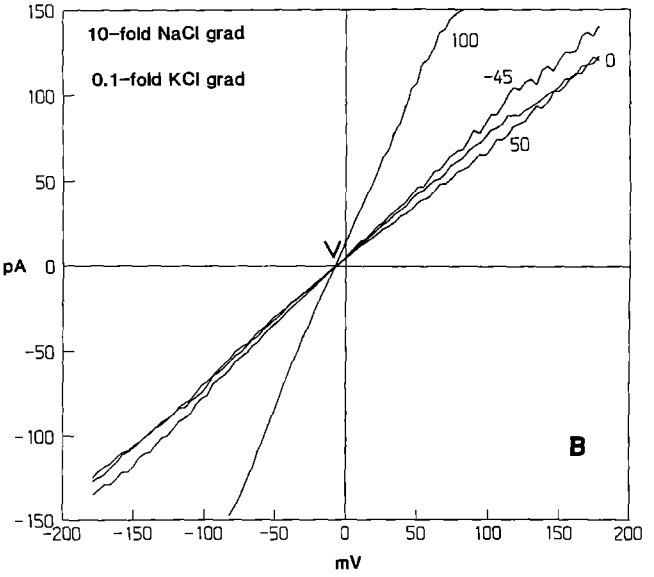

Fig. 7 A, B. Averaged current-voltage relationships of MC-LR-containing bilayers under ion gradients and different positive and negative pressures. Triangular voltage with 400 mV (pp) amplitude and 25 s period. Data averaged over 6 cycles. Ordinates, membrane current; abscissae, ramp voltage. **A**, 6-fold KCl gradient with 83 m*M* KCl in the pipette and 500 m*M* KCl in the bath. The initial voltage difference was offset in order to obtain zero current at zero pipette potential with no bilayer at the tip. 0.5 µl of 10 mg ml^{-1} DPhL/chloroform was spread over a 60 cm^2 Petri dish. Initial seal resistance was 20 GΩ, which increased up to 3 times at positive pressures. 10 ng ml^{-1} MC-LR in the pipette. No open states were seen at zero pressure. Numbers next to I/V curves indicate the pressures. *Arrow 1:* reversal voltage of the leak current at zero pressure is 19 mV; *arrow 2:* mean reversal voltage of the open state currents is 37.5 mV. **B**, 10-fold NaCl gradient, 0.1-fold KCl gradient i.e. 15 m*M* NaCl and 150 m*M* KCl in the pipette, 150 m*M* NaCl and 15 m*M* KCl in the bath. 0.6 µl of 10 mg ml^{-1} DPhL/chloroform spread over 60 cm^2 Petri dish. Seal resistance, 2 GΩ. 50 ng ml^{-1} MC-LR in the pipette. Numbers next to I/V curves indicate the pressures. Open states present at zero pressure. *Arrow:* reversal voltage of open state current is −7.7 mV

nomenon was especially striking with asymmetric ionic distributions. The current-voltage curves were also nonlinear in comparison with those obtained with symmetric ion distributions.

Experiments were also undertaken to investigate the relative permeabilities of potassium and sodium. At 150 m*M*, NaCl inside the pipette (where the toxin was also present) blocked pore formation, but at 100 m*M* pore formation occurred. A 10-fold out (bath)/in (pipette) NaCl gradient was established together with a 0.1-fold out/in KCl gradient. The Cl^- concentration was the same on either side of the membrane. Therefore, the net diffusion current at zero membrane potential depended upon the ratio of the Na and K permeabilities.

This current was positive and the reversal voltage slightly negative (Fig. 7 B), indicating that the MC-LR pore is weakly K^+ selective over Na^+. The total pore current at zero voltage (Fig. 7 B) increased with pressure (i.e. more pores opened), but the reversal voltage for this current did not change. From its average value of −7.7 mV and using the ratio $P_{Cl}/P_K = 0.175$, as calculated above, the Goldman-Hodgkin-Katz equation gives

$P_{Na}/P_K = 0.61$.

3.6 Pressure affects both the pore conductance and the kinetics of a pore

About 30 conductance levels were identified in membranes containing MC-LR. These ranged from 3 pS to 1800 pS (Fig. 12). Some appeared to be multiples of a single conductance step (Fig. 10), but in general they were not obviously related. This precludes definite conclusions concerning the number of pores in the bilayer. At low MC-LR concentrations (e.g. 10–50 ng ml^{-1}) open states were more numerous at negative voltages; at high toxin concentrations (e.g. 200 ng ml^{-1}) the opposite situation held.

The existence of numerous open conductance states hampered systematic studies of pore gating kinetics. However, when only one major open conductance state was present, the pore open-close kinetics could be studied by constructing pdfs of pore dwell times (Fig. 11). With 450 events (openings and closings) the average pore open time in Fig. 11 was 144 ms and the open time pdf was best fitted by two exponential functions, suggesting at least two substrates of each open state. The closed state kinetic data should be interpreted cautiously because the patches may have contained more than one pore despite the absence of superpositions of openings of the major conductance state in this recording.

It is worth noting that transiently-applied lateral tension sometimes dramatically changed the kinetics of a pore by switching it to a metastable, long lived open state (Fig. 5). A more frequent phenomenon during applied pressure was an increase in open state probability followed by the induction of higher conductance open states (Figs. 8, 9).

4 Discussion

The space-filled molecular model of MC-LR (Fig. 2) underlines the importance of the side chain of the β-amino

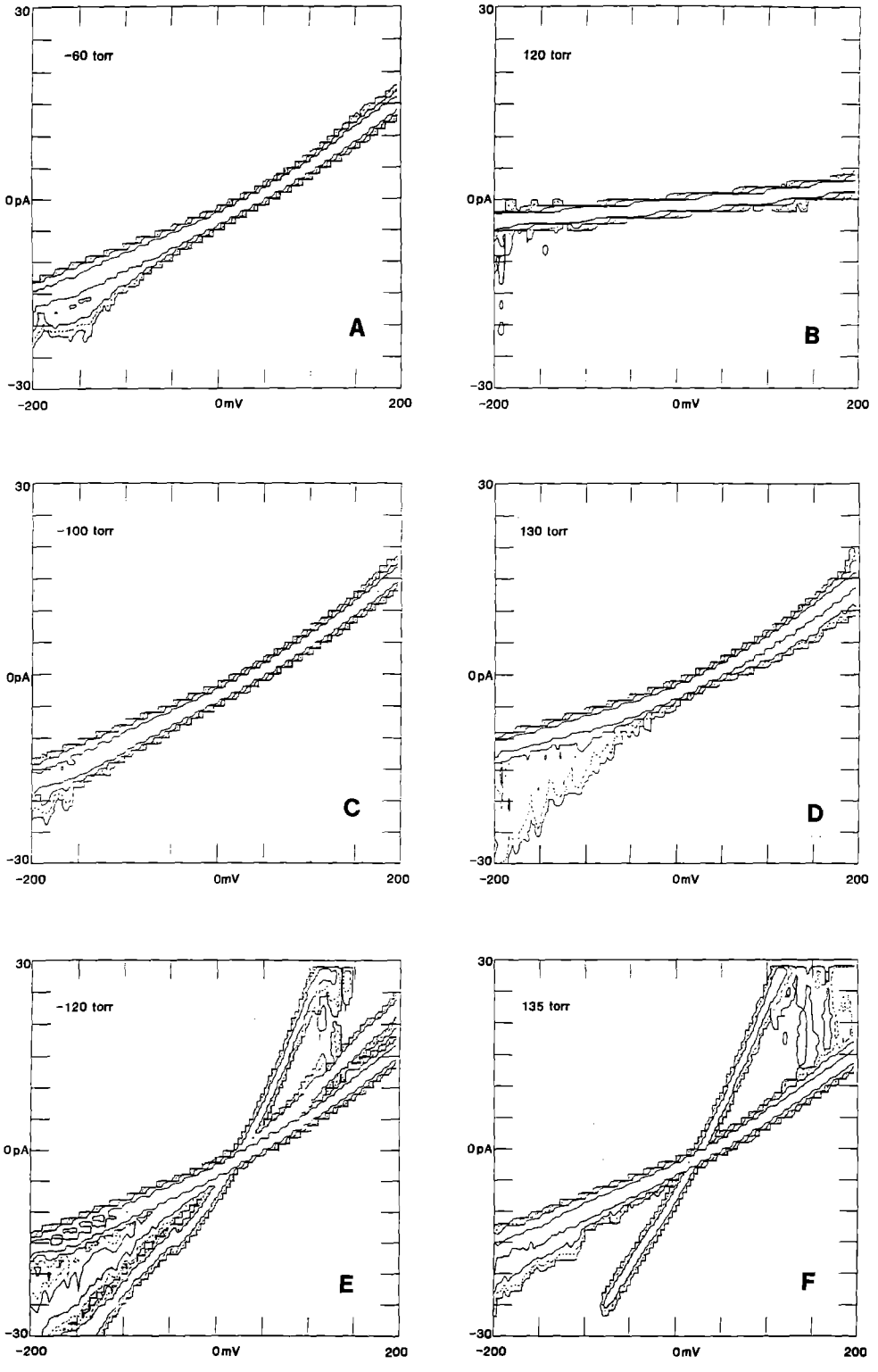

Fig. 8A–F. Opening of higher conductance states in a MC-LR-containing bilayer under positive and negative pressures; 6-fold KCl gradient. Current-voltage surfaces constructed from the same data sets as the average I/V curves in Fig. 7A. Ordinates, membrane current; abscissae, ramp voltage. Experimental conditions identical to Fig. 7A. Note the threshold-like behaviour of the openings: positive pressure threshold is 135 torr (**F**), negative pressure threshold is −120 torr (**C**). One open state of 164 pS conductance at 135 torr (**F**) and four open states of 10 pS, 55 pS, 107 pS and 160 pS at −120 torr (**C**) can be identified at negative pipette potentials. Note the tendency to switch from high conductance states to lower ones both at positive and negative potentials

acid Adda, viz., 3-amino-9-methoxy-10-phenyl-2,6,8-trimethyldeca-4,6-dienoic acid. It is this chain which gives a biphilic nature to the toxin molecule. This conclusion is supported by the surface tension measurements reported herein. In terms of the generalized molecular asymmetry model (Derzhanski and Petrov 1982; Petrov and Derzhanski 1987; Petrov 1988) MC-LR can be considered as a combination of a longitudinal biphilic dipole and a longitudinal steric (wedge-like) dipole. A comparison of the models of MC-LR and DPhL demonstrates that the lengths of their hydrophobic moieties almost match. It follows, therefore, that emplacement of MC-LR in only one half of the lipid bilayer is conceivable. However, the hydrophilic part of the toxin is bulkier than that of lecithin. Therefore, a single MC-LR molecule, with its wedge-like asymmetry, could induce strong local curvature of the adjacent lipid monolayer, a prerequisite of edge formation and pore appearance. Emplacement of

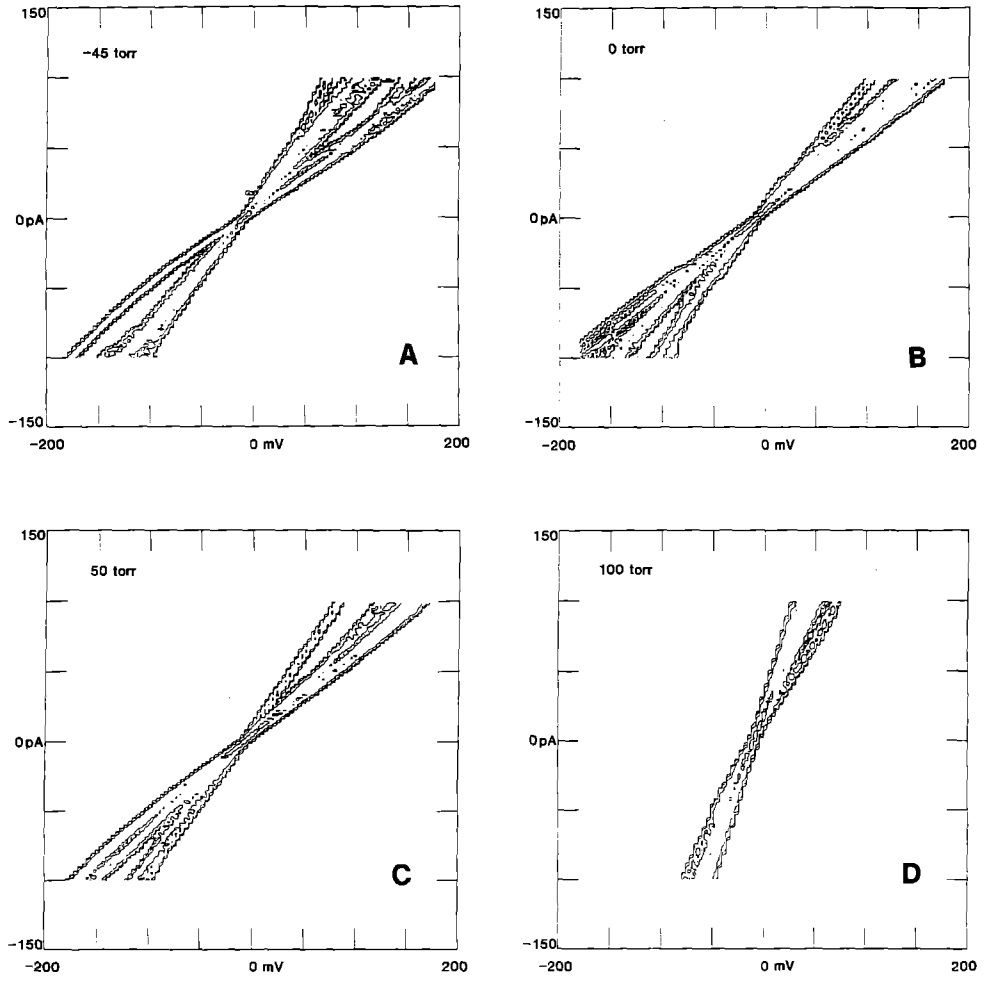

Fig. 9A–D. Opening of higher conductance states in a MC-LR-containing bilayer under negative and positive pressures; 10-fold NaCl gradient, 0.1-fold KCl gradient. Current-voltage surfaces constructed from the same data sets as the I/V curves in Fig. 7B. Ordinates, membrane current; abscissae, ramp voltage. Experimental conditions identical to Fig. 7B. Conductance states at 0 torr (**B**) and negative potentials were 55 pS, 120 pS, 200 pS and 470 pS; at −45 torr (**A**) they were 290 pS, 395 pS and 495 pS; at 50 torr (**C**) they were 115 pS, 360 pS and 465 pS; and at 100 torr (**D**) they were 615 pS and 1370 pS. Leak current also increased slightly with pressure

MC-LR with its unsaturated chain located inside the hydrophobic core of the bilayer could be anticipated and a pore-type of aggregation of the wedge-like molecules could be expected.

The aggregation of toxin monomers is a process governed by random two-dimensional diffusion of the toxin in the membrane plane. If, however, the application of transmembrane voltage and/or lateral tension cause electroporation, i.e. the formation of hydrophylic membrane pores with curved monolayer edges, then the wedge-like steric dipoles of the MC-LR molecules will be attracted by long range elastic forces (Petrov 1988) towards these edges. They will reduce the edge energy of the pore, thus effectively preventing the pore from resealing. Such pores could respond to lateral tension by increasing their radius and, eventually, recruiting more toxin molecules, which would explain the step-wise transition to higher conductance states (see Sect. 3.4). The basic difference between channel gating in native membranes and pore opening in model membranes is that in the case of pores mechanical tension not only influences open-close kinetics by lowering some potential barrier between closed and open state(s) but also induces higher pore conductance.

At neutral pH, MC-LR will carry a net negative charge. This would explain the potential dependence of toxin emplacement in the lipid bilayer. The cation selectivity of the MC-LR pore probably also arises from the negative charges present over its surface. Our finding that 150 m*M* NaCl in the toxin-containing buffer actually prevents pore formation might also explain the difference in the toxin-induced membrane permeability changes in erythrocytes and in hepatocytes (Eriksson et al. 1987); the erythrocyte experiments were performed in 145 m*M* NaCl containing buffer and revealed no pemeability changes with concentrations of toxin up to 90 μ*M*.

Negative and positive pressures seem to be equivalent with respect to pore opening formation. This shows that the effects observed are produced by membrane tension, not pressure itself. The small differences in the positive and negative pressure thresholds that were seem may be due to the different geometry (i.e. membrane curvature) in the two cases. Lack of knowledge of the patch geometry prevented us from pursuing a quantitative treatment of the tension effects. The result of attempts electronically to monitor patch area changes by phase sensitive capacitance measurements using a lock-in amplifier were inconclusive due to the small value of the patch capacitance.

The unusual voltage gating characteristics of the MC-LR pores, in which higher conductance states were initially enhanced with increasing voltage but then suppressed at high voltages, is of interest. An understanding of this phenomenon may be found in the influence of the dielectric

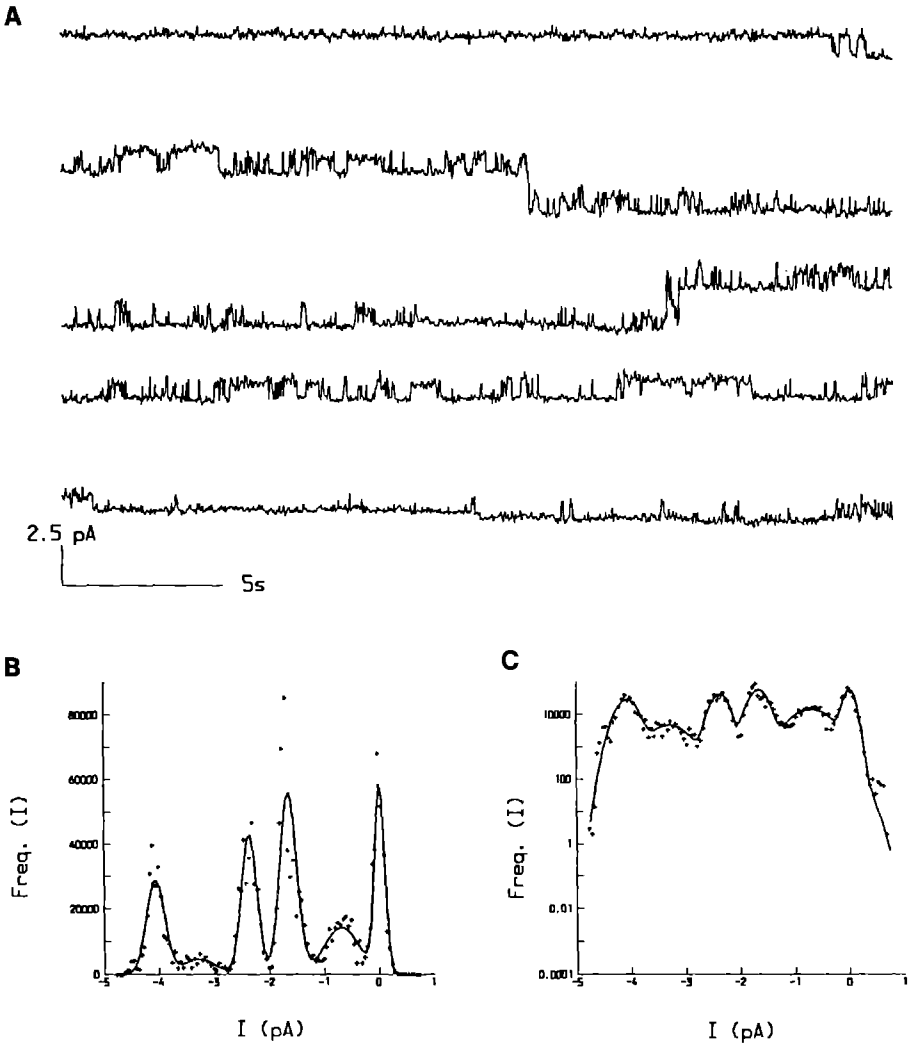

Fig. 10. Pore currents of a MC-LR containing bilayer under negative pressure of −80 torr at −150 mV (**A**) and their amplitude histograms (**B**–**C**). 6-fold KCl gradient: 83 m*M* KCl in the pipette, 500 m*M* KCl in the bath. 0.5 µl of 10 mg ml^{-1} DPhL/chloroform spread over a 60 cm^2 Petri dish. Pipette resistance, 3 *M*Ω; seal resistance, 60 GΩ. 10 ng ml^{-1} MC-LR in the pipette. Currents were 3 KHz filtered on play-back. Amplitude histogram bin width was 0.05 pA. The histogram in lin/lin form (**B**) and lin/log form (**B**) displays 6 peaks, the leftmost peaks at 0 pA being the closed state. Five open pore conductance states of 3.4 pS, 8.8 pS, 12.4 pS, 17.0 pS, and 21.2 pS were present

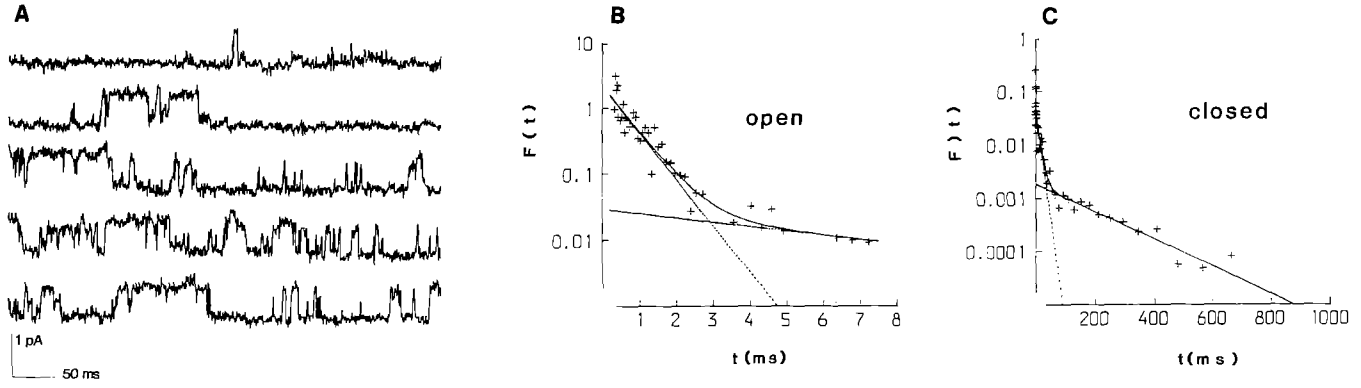

Fig. 11. Probability density functions (pdfs) of open (**B**) and closed (**C**) times of MC-LR pore of the major open state conductance of 15 pS at −80 torr and −50 mV which is illustrated in **A**. Same membrane as in Fig. 10. Current data were low-pass filtered at 3 kHz, sampled at 10 kHz and reduced to dwell time vectors using a single-threshold crossing algorithm. Open state pdf in **B** was fitted by a sum of 2 exponentials with time constants 0.6 ms and 6.6 ms. Closed state pdf in **C** was fitted by 2 exponentials with time constants 10.6 ms and 167.8 ms, although a third brief open state may also be present. Closed times should be treated with caution, since there may be more than one pore. However, there were no superpositions of the 15 pS conductance openings in the current traces exemplified in **A**

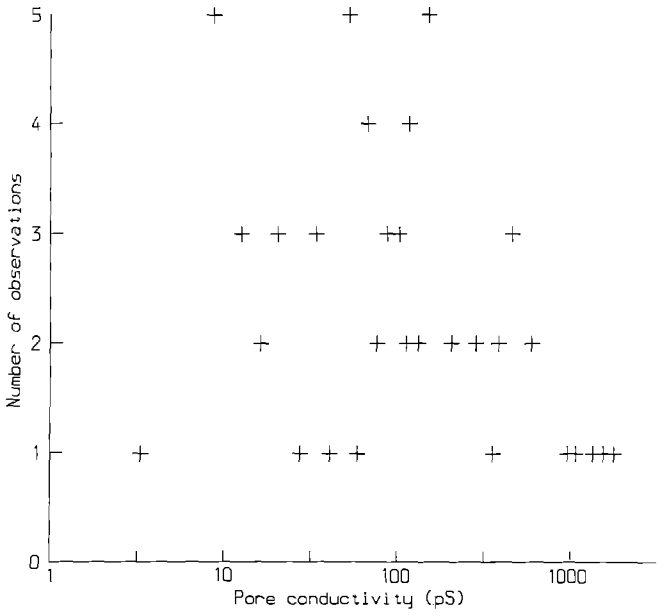

Fig. 12. Semilog scattergram of open state conductances as observed in 10 experiments with different MC-LR concentrations, tensions and voltages, identified in histograms and current voltage surfaces

ponderomotive force, which will tend to push apart the pore walls when water molecules are attracted into the pore interior (Chernomordik and Chizmadzhev 1989), and the overall decrease of bilayer tension in an electric field as predicted by the Lippmann equation. The latter can be understood qualitatively in terms of an increase in lateral repulsion along the membrane surface as the charge stored in the membrane capacity is increased (Requena et al. 1975). Both of these influences on the voltage gating characteristics are proportional to the square of the electric field, i.e. the transmembrane voltage. The ponderomotive force prevails for small pores, but for larger ones where the electric field in the pore centre is negligibly small, it falls to a value which is about 50% of Lippmann force (Sugar 1989). This ponderomotive force is more influential at high ionic strengths, since the shorting out of the field in the pore centre takes place at lower radii, i.e. at lower pore conductance (cf. Fig. 6 and Fig. 8).

An attractive feature of these findings is that both the mechanical and electric components of the lateral membrane tension could be involved and, correspondingly utilised, in pore switching.

5 Conclusion

The cyanobacterial toxin, MC-LR induces mechanosensitive ion pores in fluid lipid membranes. This system offers a useful model of mechanosensitivity phenomena in native membranes. The results of this study also point the way towards a possible use of a liquid crystal lipid matrix containing monomers of pore-forming molecules in mechanical sensors and molecular switches, thus providing a further application of the guest-host liquid crystal concept in molecular electronics.

Acknowledgements. AGP and PNRU were supported by the UK SERC (GR/F 15243) and AGP also by the Bulgarian Ministry of Science and Higher Education (Project No. 587). GAC thanks the Royal Society for support. Thanks are due to Mr. C. Standley for technical assistance in Nottingham, to Mr. K. A. Beattie and Miss L. A. Lawton for technical assistance in Dundee and to Dr. M. Sansom and Mr. I. Mellor for introducing us to the current-voltage surfaces software.

References

Albrecht O, Gruler H, Sakmann E (1978) Polymorphism of lipid monolayers. J Phys 39:301–313

Botes DP, Wessels PL, Kruger H, Runnegar MTC, Santikarn S, Smith RJ, Barna JCJ, Williams DH (1985) Structural studies on cyanoginosins-LR, -YR, -YA and YM, peptide toxins from *Microcystis aeruginosa*. J Chem Soc Perkin Trans 1:2747–2748

Brehm P, Kullberg R, Moody-Corbett F (1984) Properties of non-junctional acetylcholine receptor channels on innervated muscle of *Xenopus laevis*. J Physiol 350:631–648

Brooks WP, Codd GA (1986) Extraction and purification of toxic peptides from natural blooms and laboratory isolates of the cyanobacterium *Microcystis aeruginosa*. Lett Appl Microbiol 2:1–3

Carmichael WW (1989) Freshwater cyanobacteria (blue-green algae) toxins. In: Ownby SL, Odell GV (eds) Natural toxins. Characterization, pharmacology and therapeutics. Pergamon Press, Oxford, pp 3–16

Chernomordik LV, Chizmadzhev YA (1989) Electrical breakdown of lipid bilayer membranes. In: Neumann E, Sowers AE, Jordan CA (eds) Eletroporation and electrofusion in cell biology. Plenum Press, New York, pp 83–95

Codd GA, Brooks WP, Lawton LA, Beattie KA (1989 a) Cyanobacterial toxins in European waters: occurrence, properties, problems and requirements. In: Wheeler D, Richardson MJ, Bridges J (eds) Watershed 89. The future for water quality in Europe, vol II. Pergamon Press, Oxford, pp 211–220

Codd GA, Brooks WP, Priestley IM, Poon GK, Bell SG, Fawell JK (1989 b) Production, detection and quantification of cyanobacterial toxins. Toxicity Assess 4:499–511

Corey DP, Hudspeth JA (1983) Kinetics of the receptor current in bullfrog saccular hair cells. J Neurosci 3:962–976

Corronado R, Latorre R (1983) Phospholipid bilayers made from monolayers on patch-clamp pipettes. Biophys J 43:231–236

Derzhanski A, Petrov AG (1982) Multipole model of the molecular asymmetry in thermotropic and lyotropic liquid crystals. Mol Cryst Liq Cryst 89:339–360

Edwards C, Ottoson D, Rydqvist B, Swerup C (1981) The permeability of the transducer membrane of the crayfish stretch receptor to calcium and other divalent ions. Neuroscience 6:1455–1460

Eriksson JE, Haegerstrand H, Isomaa B (1987) Cell selective cytotoxicity of a peptide toxin from the cyanobacterium *Microcystis aeruginosa*. Biochim Biophys Acta 930:304–310

Eriksson JE, Meriluoto JAO, Kujari HP, Jamel Al-Layl K, Codd GA (1988) Cellular effects of cyanobacterial peptide toxins. Toxicity Assess 3:511–517

Eriksson JE, Paatero GIL, Meriluoto JAO, Codd GA, Kass GEN, Nicotera P, Orrenius S (1989) Rapid microfilament reorganization induced in isolated rat hepatocytes by microcystin-LR, a cyclic peptide toxin. Exp Cell Res 185:86–100

Exerowa D, Kashchiev D (1986) Hole-mediated stability and permeability of bilayers. Contemp Phys 27:429–461

Falconer IR, Runnegar MTC (1987) Effects of the peptide toxin from *Microcystis aeruginosa* on intracellular calcium, pH and membrane integrity in mammalian cells. Chem Biol Interact 63:215–225

Guharay F, Sachs F (1984) Stretch-activated single ion channel currents in tissue-cultured embryonic chick skeletal muscle. J Physiol 352:685–701

Hille B (1984) Ionic channels of excitable membranes, Sinauer, Sunderland Mass

Katz B (1950) Depolarization of sensory terminals and the initiation of impulses in the muscle spindle. J Physiol 111:261–282

Kerry CJ, Kits KS, Ramsey RL, Sansom MSP Usherwood PNR (1987) Single channel kinetics of a glutamate receptor. Biophys J 51:137–144

Krishnamurthy T, Szafraniec L, Hunt DF, Shabanowitz J, Yates JR, Hauer CR, Carmichael WW, Skulberg O, Codd GA, Missler S (1989) Structural characterization of toxic cyclic peptides from blue-green algae by tandem mass spectrometry. Proc Natl Acad Sci USA 86:770–774

Lindsey H, Petersen NO, Chan SI (1979) Physicochemical characterization of 1,2-diphytanoyl-sn-glycero-3-phosphocholine in model membrane systems. Biochim Biophys Acta 555:147–167

Mellor IR, Thomas DH, Sansom MSP (1988) Properties of ion channels formed by *Staphylococcus aureus* δ-toxin. Biochim Biophys Acta 942:280–284

Morris CE (1990) Mechanosensitive ion channels. J Membrane Biol 113:93–107

Morris CE, Sigurdson WJ (1989) Stretch-inactivated ion channels coexist with stretch-activated ion channels. Science 243:807–809

Passechnik VI, Sokolov VS (1973) Permeability change of modified bimolecular phospholipid membranes accompanying periodical expansion. Biofizika (Moscow) 18:655–660

Pastushenko VF, Petrov AG (1984) Electromechanical mechanism of pore formation in bilayer lipid membranes. Seventh School Biophys. Membrane Transport, Poland, School Proceedings, Wroclaw, vol 2, pp 69–91

Petrov AG (1988) Generalized lipid asymmetry and instability phenomena in membranes. Ninth School on Biophysics of Membrane Transport. School Proceedings, Wroclaw, Poland, vol 2, pp 67–86

Petrov AG, Derzhanski A (1987) Generalized asymmetry of thermotropic and lyotropic mesogens. Mol Cryst Liq Cryst 151:303–333

Petrov AG, Mitov MD, Derzhanski A (1980) Edge energy and pore stability in bilayer lipid membranes. In: Bata L (ed) Advances in liquid crystal research and applications. Pergamon Press, Oxford, Akad. Kiado, Budapest, pp 695–737

Requena J Haydon DA, Hladki SB (1975) Lenses and the compression of black lipid membranes by an electric field. Biophys J 15:77–81

Sachs F (1986) Mechanotransducing ion channels. In: Latorre R (ed) Ionic channels in cells and model systems. Plenum Press, London, pp 181–193

Sachs F (1988) Mechanical transduction in biological systems. CRC Crit Rev Biomed Eng 16:141–169

Sakmann B, Neher E (1983) Geometric parameters of pipettes and membrane patches. In: Sakmann B, Neher E (eds) Single-channel recordings. Plenum Press, New York London, pp 37–51 (Figs. 2–8)

Sansom MSP, Mellor IR (1990) Analysis of the gating of single ion channels using current-voltage surfaces. J Theor Biol 114:213–223

Sugar IP (1989) Stochastic model of electric field-induced membrane pores. In: Neumann E, Sowers AE, Jordan CA (eds) Electroporation and electrofusion in cell biology, Plenum Press, New York London, pp 97–110